Ophthalmic Research

Research Article

Ophthalmic Res 2023;66:228–237
DOI: 10.1159/000526370

Received: June 13, 2022
Accepted: July 28, 2022
Published online: September 28, 2022

Characterization of 2-Year Progression of Different Phenotypes of Nonproliferative Diabetic Retinopathy

Luísa Ribeiro[a, b, c] Inês P. Marques[a, b, c] Torcato Santos[a] Sara Carvalho[a] Ana R. Santos[a, b, c, d] Luís Mendes[a] Conceição Lobo[a, b, c, e] José Cunha-Vaz[a, b, c]

[a]AIBILI – Association for Innovation and Biomedical Research on Light and Image, Coimbra, Portugal; [b]Faculty of Medicine, Coimbra Institute for Clinical and Biomedical Research (iCBR), University of Coimbra, Coimbra, Portugal; [c]Center for Innovative Biomedicine and Biotechnology (CIBB), University of Coimbra, Coimbra, Portugal; [d]Department of Orthoptics, School of Health, Polytechnic of Porto, Porto, Portugal; [e]Department of Ophthalmology, Centro Hospitalar e Universitário de Coimbra (CHUC), Coimbra, Portugal

Keywords
Retina · Diabetic retinopathy · Diabetic macular edema · Neurodegeneration · Retinal ischemia

Abstract

Introduction: The aim of the study was to characterize the 2-year progression of risk phenotypes of nonproliferative diabetic retinopathy (NPDR) in type 2 diabetes (T2D) phenotype C, or ischemic phenotype, identified by decreased skeletonized retinal vessel density (VD), ≥2 SD over normal values, and phenotype B, or edema phenotype, identified by increased retinal thickness, i.e., subclinical macular edema, and no significant decrease in VD. ***Methods:*** A prospective longitudinal cohort study (CORDIS, NCT03696810) was conducted with 4 visits (baseline, 6 months, 1 year, and 2 years). Ophthalmological examinations included best-corrected visual acuity, color fundus photography (CFP), and optical coherence tomography (OCT) and OCT angiography. Early Treatment Diabetic Retinopathy Study grading was performed at the baseline and last visits based on 7-field CFP. ***Results:*** One hundred and twenty-two eyes from T2D individuals with NPDR fitted in the categories of phenotypes B and C and completed the 2-year follow-up. Sixty-five (53%) of the eyes were classified as phenotype B and 57 (47%) eyes as phenotype C. Neurodegeneration represented by thinning of the ganglion cell layer and inner plexiform layer was present in both phenotypes and showed significant progression over the 2-year period ($p < 0.001$). In phenotype C, significant progression in the 2-year period was identified in decreased skeletonized VD ($p = 0.01$), whereas in phenotype B microvascular changes involved preferentially decrease in perfusion density (PD, $p = 0.012$). Phenotype B with changes in VD and PD (flow) and preferential involvement of the deep capillary plexus ($p < 0.001$) is associated with development of center-involved macular edema. ***Discussion:*** In the 2-year period of follow-up, both phenotypes B and C showed progression in retinal neurodegeneration, with changes at the microvascular level characterized by decreases in PD in phenotype B and decreases in VD in phenotype C.

Karger@karger.com
www.karger.com/ore

Correspondence to:
José Cunha-Vaz, cunhavaz@aibili.pt

Introduction

Diabetic retinopathy (DR) is a frequent complication of diabetes and through its vision-threatening complications, i.e., macular edema and proliferative retinopathy, may lead to blindness. DR is also the leading cause of vision loss in working age adults [1, 2].

We have identified three different phenotypes of nonproliferative DR (NPDR) with different risks for progression and development of sight-threatening complications [3–5]. One, phenotype C, representing 25% of the eyes with NPDR, is characterized by the presence of active microvascular disease identified by increased microaneurysm turnover (MAT) above a specified level. Phenotype B, representing another 25% of the eyes with NPDR, is characterized by low levels of MAT and the presence of subclinical macular edema. Finally, phenotype A, representing 50% of the eyes, is characterized by low levels of MAT and absence of subclinical macular edema. This phenotype over a 5-year period showed little progression and no vision-threatening complications [5]. Considering that MAT is not widely used and that microvascular disease can be quantified noninvasively by optical coherence tomography angiography (OCTA), we have replaced MAT metrics by definitive changes in retinal vessel density (VD), i.e., VD decrease in the retinal superficial capillary plexus (SCP) of ≥2 standard deviation (SD) of a healthy control population to identify phenotype C, the ischemic phenotype.

Only patients with NPDR and risk phenotypes B and C were included in a prospective longitudinal study and followed for a period of 2 years, with the objective of characterizing patterns of progression of NPDR, looking for eyes that show evidence of active disease and are at a higher risk of progression and development of complications. This goal is of major relevance for the design of future clinical trials to test new drugs and to identify the patients at risk for disease progression and in need for increased surveillance.

Methods

This prospective longitudinal observational cohort study CORDIS (ClinicalTrials.gov identifier Number NCT03696810) was designed to conduct a 2-year follow-up study in individuals with type 2 diabetes (T2D) and with NPDR (levels 20, 35, 43, and 47, in the Early Treatment Diabetic Retinopathy Study (ETDRS) severity scale) to characterize this population at demographic, systemic, and ophthalmological level. The tenets of the Declaration of Helsinki were followed, and the study was reviewed and approved by the Ethics Committee of AIBILI with the number CEC/194/18 (CORDIS). A written informed consent was signed by all individuals, agreeing to participate in the study, after all procedures were explained.

Individuals were included according to specific inclusion criteria, being also classified as phenotype B or C of DR and followed for four visits: baseline (V1), 6 months (V2), 12 months (V3), and 24 months (V4). The study exclusion criteria comprised the presence of age-related macular degeneration, glaucoma, vitreomacular disease, high ametropia (spherical equivalent greater than −6 and +2 D), any previous laser treatment or intravitreal injections, or any patient comorbidity likely to affect the eye and not related to diabetes, renal or cardiovascular disease. This information was obtained through their medical assistant. Concomitant medication was also registered to confirm this information. Excluded were also T2D patients with uncontrolled systemic hypertension (values outside normal range: systolic 70–210 mm Hg and diastolic 50–120 mm Hg), hemoglobin A1c (HbA1c) levels above 10%, during the first 6 months of the study, and a history of ischemic heart disease. Eyes with baseline central thickening identifying center-involved macular edema (CIME), defined as a central retinal thickness (CRT) ≥ 290 μm in women and ≥305 μm in men [6], were also excluded.

Visual acuity (best-corrected visual acuity [BCVA]) was measured for each eye using the ETDRS protocol and precision vision chart at 4 m [7]. A total of 128 people with T2D were enrolled in the study, but the data analysis considered only 122 eyes that fulfilled the criteria for classification as phenotypes B and C (Fig. 1), men (93, 76%), and women (29, 24%) with diagnosed adult onset of T2D, aged 47–79 years (Table 1).

At baseline visit (V1), demographics such as age, duration of diabetes, comorbidities, and concomitant medication were collected for each participant. Physical assessment with biometric measures (body weight and height) and blood pressure evaluation were performed by an experienced nurse. Laboratory analyses included plasma concentrations of HbA1c, lipid fractionation identifying total cholesterol, high-density lipoprotein (HDL), low-density lipoprotein (LDL), and triglycerides, measured to assess metabolic control.

Participants underwent a complete eye examination, which included BCVA, slit-lamp examination, color fundus photography (CFP), optical coherence tomography (OCT), and OCTA. The study eye was selected, based on the inclusion/exclusion criteria and classification as phenotypes B and C.

The calculation of the sample size was based on previous studies, where the existence of three distinct phenotypes of DR progression in T2D was identified [5]. An age-matched healthy control population of 65 individuals was used as reference for demographic and ocular variables. Data analysis was performed based on phenotype characterization based on VD decrease of the SCP ≥2 SD obtained using OCTA (phenotype C) and increased value of CRT obtained using OCT and no decrease in VD of the SCP ≥2 SD (phenotype B).

BCVA Evaluation

BCVA was assessed and recorded as letters read at 4 m on ETDRS charts. Final BCVA letter score was calculated by adding the number of letters read at 4 m plus 30 (or the number of letters read at 1 m). BCVA was evaluated using the Snellen scale and converted into logarithm units of the minimal angle of resolution (logMAR). The presence of any visual loss was recorded.

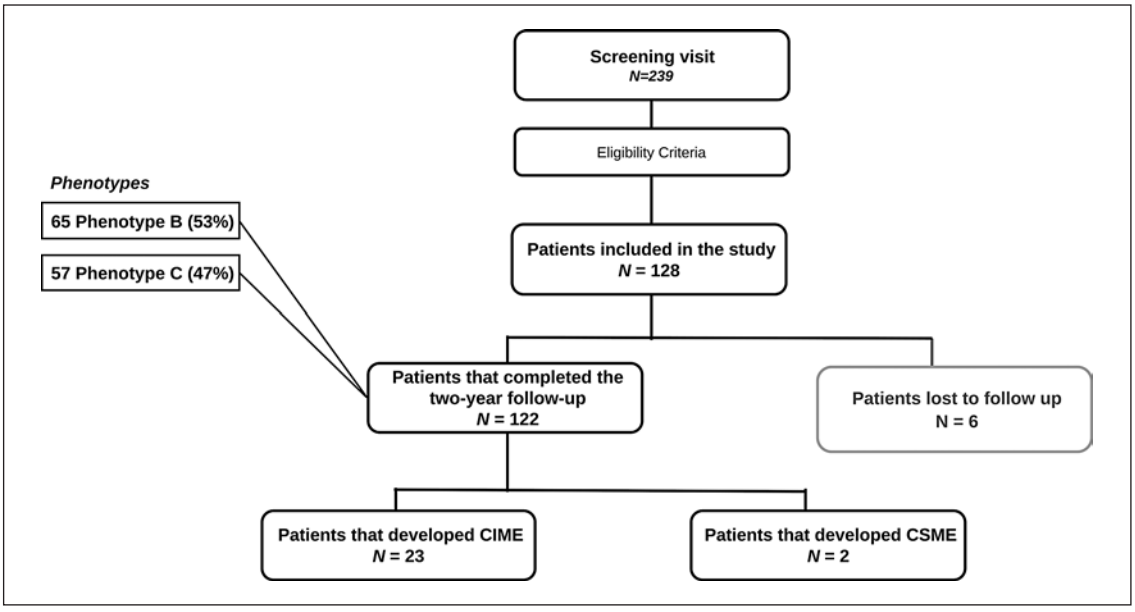

Fig. 1. Cohort flowchart. Composition of the included patients over the study period. CIME, center-involved macular edema; CSME, clinical-significant macular edema.

CFP, ETDRS, and Microaneurysm Assessment

ETDRS classification was performed based on 7-field CFP images obtained at 30/35°, using a Topcon TRC 50DX camera (Topcon Medical Systems, Tokyo, Japan), with a resolution of 3,596 × 2,448 pixels. ETDRS grading scale and the DR severity score were classified at Coimbra Ophthalmology Reading Center (CORC), using a modified Airlie House classification scheme according to the ETDRS protocol. Classification was performed by two graders, with an inter-grader agreement of 93.7% [8].

MAT was automatically performed on 45/50° 2-field images using the RetmarkerDR (Retmarker SA, Coimbra, Portugal), a computer-aided diagnostic software that performs microaneurysm (MA) earmarking and identification of macular red dot-like vascular lesions and allows the comparison of the same eye within the same retinal location between different visits. Likewise, this algorithm computes the number and localization of MA in each visit, allowing the calculation of the MA disappearance and formation rates between visits. MAT is processed as the sum of the MA formation and disappearance rates.

OCT and OCT Angiography

OCT was performed in each participant, at each visit, using the Cirrus Zeiss 5000 AngioPlex (Carl Zeiss Meditec, Dublin, CA, USA), using the acquisition protocol macular cube 512 × 128 (128 B-scans with 512 A-scans each). CRT and average ganglion cell layer + inner plexiform layer (GCL + IPL), at the inner ring (IR), were automatically collected from Zeiss Cirrus standard reports. Decrease (thinning) in GLP + IPL was considered to identify neurodegeneration.

To collect VD metrics on OCTA recordings, the 3×3 mm^2 acquisition protocol was performed over a $3 \times 3 \times 2$ mm^3 volume in the central macula, consisting of a set of 245 clusters of 4 B-scans repetitions, where each B-scan consists of 245 A-scans. Retinal perfusion density (PD) and VD at the IR and foveal avascular zone (FAZ), detected at the SCP, deep capillary plexus (DCP), and full retina (FR), were calculated using the Carl Zeiss Meditec Density Exerciser (version: 10.0.12787; Carl Zeiss Meditec, Inc.). The area of intercapillary spaces (AIS) was calculated using a method previously described by our group [9]. Morphological operations that include the bottom-hat transform were applied to the binary slab of the en face slabs generated by the Carl Zeiss Meditec Density Exerciser. AIS was computed for the SCP, DCP, and FR [9]. Quality check and normalization of signal strength were performed in all OCTA examinations [10].

Characterization of DR Phenotypes

Classification of DR phenotype for each participant was performed on VD values of the SCP and CRT according to the following rules: phenotype C, by decreased VD of SCP ≥2 SD of a reference healthy population and phenotype B by the presence of subclinical macular edema, i.e., increased CRT ≥260 μm in women and ≥275 μm in men, without decreased values of VD of SCP (<2 SD of a reference healthy population). CRT reference values presented in this study are the reference for Zeiss Cirrus 5000 SD-OCT [11]. As mentioned above, for inclusion criteria, only individuals classified with phenotype B or C were analyzed in study (Fig. 2).

Statistical Analysis

Data on each eye/patient are represented as means and corresponding SDs for continuous variables and absolute and relative frequencies for categorical and ordinal variables. Accordingly, a comparison of baseline characteristics between overall participants and healthy controls was performed using the Mann-Whit-

Table 1. Comparison of baseline demographics, systemic, and ocular characteristics between patients that completed the study and healthy controls and between different phenotypes

	Patients (*N* = 122)	Healthy (*N* = 65)	*p* value (patients vs. healthy)	Phenotype B (*N* = 65)	Phenotype C (*N* = 57)	*p* value (phenotype B vs. phenotype C)
Demographic characteristics						
Gender, male/female, *n* (%)	93/29 (76.2/23.8)	35/30 (53.8/46.2)		52/13 (80.0/20.0)	41/16 (71.9/28.1)	
Age, mean ± SD, years	67.12±6.66	67.26±2.72	0.355	67.57±6.53	66.61±6.84	0.488
Diabetes duration, mean±SD, years	19.61±7.4			19.75±8.15	19.44±6.51	0.909
Severity levels, n (%)						
ETDRS level 20	12 (9.8)			9 (13.8)	3 (5.3)	
ETDRS level 35	74 (60.7)			40 (61.5)	34 (59.6)	
ETDRS level 43–47	36 (29.5)			16 (24.6)	20 (35.1)	
Systemic characteristics, mean ± SD						
BMI, kg/m^2	29.29±4.06			28.59±3.97	30.08±4.05	**0.010**
HbA1c, %	7.7±1.4			7.55±1.16	7.86±1.62	0.363
Total cholesterol, mg/dL	161.64±41.83			162.6±43.74	160.54±39.9	0.972
LDL cholesterol, mg/dL	90.56±33.05			89.98±34.4	91.21±31.72	0.612
HDL cholesterol, mg/dL	45.34±11.52			47.08±10.17	43.35±12.68	**0.023**
Triglycerides, mg/dL	128.83±63.14			127.71±62.52	130.11±64.38	0.873
Systolic blood pressure, mm Hg	138.93±11.69			139.8±12.69	137.93±10.46	0.120
Diastolic blood pressure, mm Hg	72.82±8.57			74.12±8.73	71.33±8.21	0.090
Ocular characteristics, mean ± SD						
BCVA, logMAR	0.01±0.08			0.00±0.08	0.03±0.09	0.218
MA turnover 6 months	4.9±6.3			3.69±6.72	6.31±5.60	**<0.001**
CRT, µm	277.7±19.5	260.6±18.3	**<0.001**	285.6±13.1	268.8±21.8	**<0.001**
GCL + IPL thickness, µm	80.1±7.49	82.7±5.5	**0.032**	81.4±6.9	78.7±7.7	0.069
FAZ circularity	0.59±0.10	0.65±0.06	**<0.001**	0.60±0.1	0.58±0.11	0.529
FAZ area, mm^2	0.24±0.09	0.24±0.10	0.952	0.22±0.1	0.25±0.09	**0.026**
VD – IR – SCP, mm^{-1}	20.62±1.32	22.35±0.87	**<0.001**	21.63±0.71	19.6±0.94	**<0.001**
VD – IR – DCP, mm^{-1}	15.8±2.16	17.26±2.16	**<0.001**	16.78±1.60	14.82±2.22	**<0.001**
VD – IR – FR, mm^{-1}	22.34±1.25	23.75±0.9	**<0.001**	23.25±0.73	21.43±0.97	**<0.001**
PD – IR – SCP	0.39±0.02	0.40±0.02	**<0.001**	0.40±0.02	0.38±0.02	**<0.001**
PD – IR – DCP	0.31±0.04	0.33±0.04	**<0.001**	0.32±0.03	0.29±0.04	**<0.001**
PD – IR – FR	0.42±0.02	0.42±0.02	**0.013**	0.43±0.02	0.40±0.02	**<0.001**
AIS – SCP (×1,000)	28.69±10.92	11.60±3.18	**<0.001**	23.02±10.06	34.35±8.61	**<0.001**
AIS – DCP (×1,000)	43.84±14.91	27.80±8.95	**<0.001**	39.25±14.11	48.43±14.36	**<0.001**
AIS – FR (×1,000)	18.43±7.99	7.52±2.62	**<0.001**	15.01±7.56	21.86±6.91	**<0.001**

Bold values represent statistically significant alterations with $p < 0.05$ using the Mann-Whitney test. *n*, number of participants; SD, standard deviation; ETDRS, Early Treatment Diabetic Retinopathy Study; BMI, body mass index; HbA1c, glycated hemoglobin A1c; LDL, low-density lipoprotein; HDL, high-density lipoprotein; BCVA, best-corrected visual acuity; CRT, central retinal thickness; GCL + IPL, ganglion cell layer + inner plexiform layer; FAZ, foveal avascular zone; SCP, superficial capillary plexus; DCP, deep capillary plexus; FR, full retina; IR, inner ring; PD, perfusion density; AIS, area of intercapillary space.

ney test, given that data were not normally distributed. The Mann-Whitney test was also applied to analyze changes in baseline, 1-year and 2-year follow-up characteristics, between phenotypes, and changes in characteristics between patients presenting and not presenting CIME at the last visit. Changes in systemic and ocular characteristics at 1-year and 2-year follow-up were assessed with the Wilcoxon signed-rank test.

Data normality was assessed with the Shapiro-Wilk test. All statistical analyses were performed with Stata 16.1 (StataCorp LLC, College Station, TX, USA), and p values <0.05 were considered statistically significant.

Results

One hundred twenty-two eyes from individuals with T2D completed the 2-year follow-up. At baseline, there were 12 eyes classified as ETDRS 20, 74 eyes classified as ETDRS 35, and 36 identified as ETDRS 43–47. Of these, 57 (47%) were classified as phenotype C, identified by the presence of a decrease in VD of the SCP equal or greater to 2 SD of a normal population, and 65 (53%) were classified as phenotype B, identified by not having a decrease

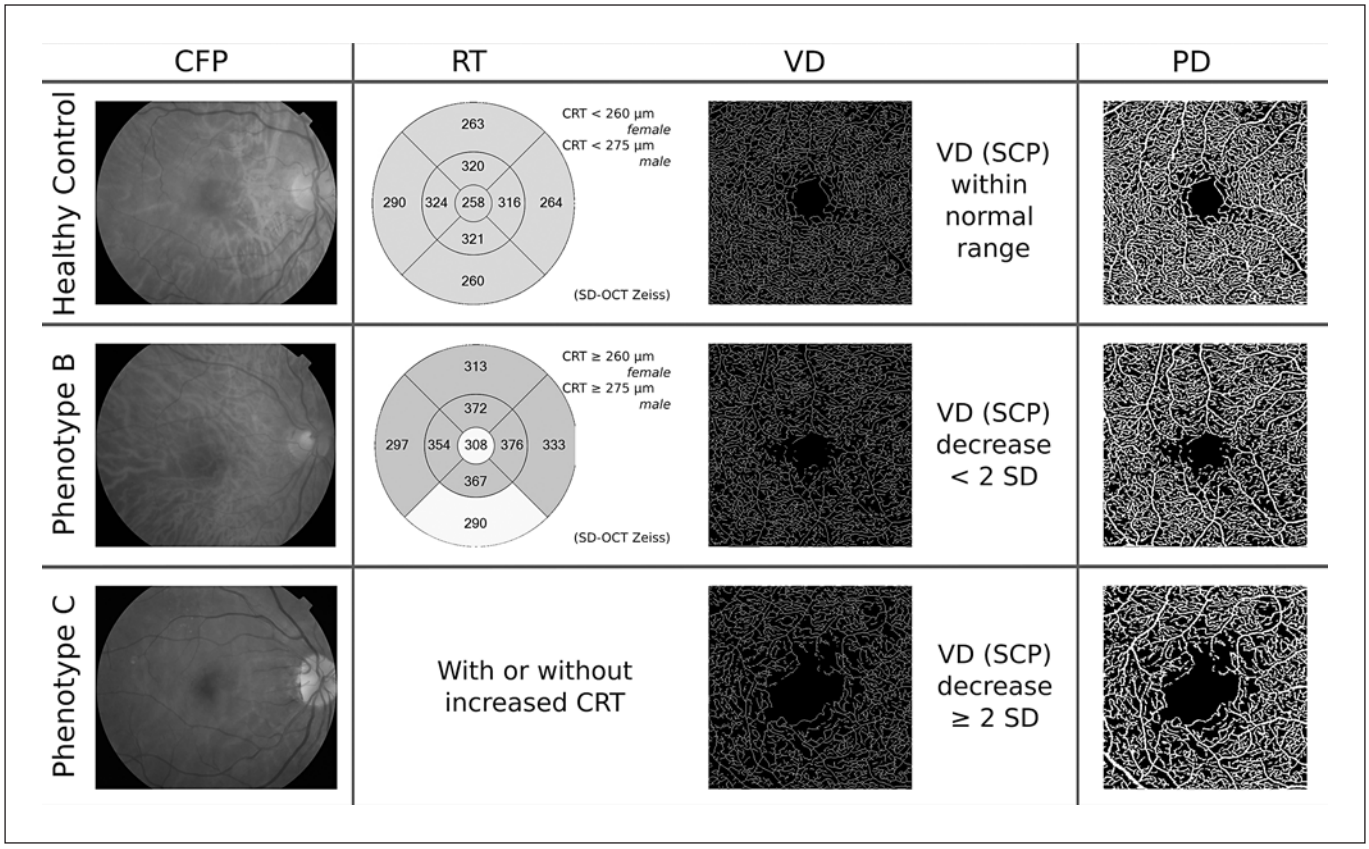

Fig. 2. Phenotype classification. Representative cases for a healthy control volunteer (top row), phenotype B patient (middle row), and phenotype C patient (bottom row). Phenotype classification is based on retinal thickness (RT, second column) to assess edema and vessel density (VD, third column) to assess ischemia. Corresponding color fundus photography (CFP, first column) and perfusion density (PD) map are included for illustrative purposes.

in VD of the SCP (2 SD comparing to a healthy control population) and increased CRT. According to the rules of phenotype classification, during the period of 2 years, of the 23 T2D eyes that developed CIME, 20 eyes were classified as phenotype B and three eyes as phenotype C. Two eyes developed clinical-significant macular edema (CSME), one in each phenotype.

Demographic, systemic, and ocular characteristics of the entire population enrolled in this study are described in Table 1. Analysis of the data collected shows that the eyes included in the study, with only minimal, mild, and moderate NPDR, show, as a whole, increased CRT ($p < 0.001$), thinning of the GCL + IPL demonstrating retinal neurodegenerative changes ($p = 0.032$), altered FAZ circularity ($p < 0.001$), decreased skeletonized VD ($p < 0.001$), and PD (PD-SCP and PD-DCP, $p < 0.001$) and markedly increased AIS ($p < 0.001$).

The population distribution at baseline by phenotype, gender, age, and diabetes duration indicated no significant differences (Table 1). The characterization of each phenotype at baseline (except MAT, which was defined at a 6-month visit) is also described in Table 1. Phenotype C presented higher values of body mass index ($p = 0.01$) and lower values of HDL cholesterol ($p = 0.023$) without statistically significant differences being observed in HbA1c values, blood pressure levels, total and LDL cholesterol, and triglycerides between the two different phenotypes populations (Table 1), confirming that the study population was generally well controlled as per inclusion criteria.

In agreement with the criteria for definition of DR phenotypes, CRT was increased in phenotype B when compared to phenotype C ($p < 0.001$), likewise, phenotype C presented significant decreases of OCTA metrics

Table 2. Overall 2-year progression of the study population

	Baseline (V1 – 0M)	Two years (V4 – 24M)	Mean differences (V4-V1)	*p* value (V1 vs. V4)
Systemic characteristics, mean ± SD				
HbA1c, %	7.7±1.4	7.6±1.0	−0.1±1.1	0.900
Total cholesterol, mg/dL	161.6±41.8	156.5±36.5	−5.1±32.4	0.212
LDL cholesterol, mg/dL	90.6±33.0	81.6±29.9	−9.0±27.2	**<0.001**
HDL cholesterol, mg/dL	45.3±11.5	49.0±13.4	3.7±9.9	**<0.001**
Triglycerides, mg/dL	128.8±63.1	137.7±70.1	8.9±54.5	**0.023**
Systolic blood pressure, mm Hg	138.9±11.7	141.5±13.5	2.5±15.1	0.149
Diastolic blood pressure, mm Hg	72.8±8.6	73.9±9.6	1.0±11.1	0.396
Ocular characteristics, mean ± SD				
BCVA, logMAR	0.01±0.08	0.03±0.11	0.02±0.09	0.064
CRT, µm	277.7±19.5	279.7±26.7	2.0±17.5	0.865
GCL + IPL thickness, µm	80.1±7.4	78.7±7.6	−1.3±2.0	**<0.001**
FAZ circularity	0.59±0.10	0.61±0.08	0.00±0.09	0.535
FAZ area, mm^2	0.24±0.09	0.24±0.09	0.00±0.03	0.101
VD – IR – SCP, mm^{-1}	20.6±1.3	20.5±1.4	−0.1±1.1	0.613
VD – IR – DCP, mm^{-1}	15.8±2.2	15.4±2.2	−0.4±2.0	**0.047**
VD – IR – FR, mm^{-1}	22.3±1.3	22.4±1.3	0.1±1.1	0.430
PD – IR – SCP	0.39±0.02	0.38±0.02	−0.01±0.02	**0.001**
PD – IR – DCP	0.31±0.04	0.30±0.04	−0.01±0.03	0.068
PD – IR – FR	0.42±0.02	0.41±0.02	−0.01±0.02	**0.011**
AIS – SCP (×1,000)	28.69±10.92	29.60±12.26	0.88±8.71	0.272
AIS – DCP (×1,000)	43.84±14.91	46.37±17.44	2.69±17.13	**0.040**
AIS – FR (×1,000)	18.43±7.99	18.82±9.06	0.35±6.82	0.531

Bold values represent statistically significant alterations with $p < 0.05$ using the Wilcoxon signed-rank test. SD, standard deviation; HbA1c, glycated hemoglobin A1c; LDL, low-density lipoprotein; HDL, high-density lipoprotein; BCVA, best-corrected visual acuity; CRT, central retinal thickness; GCL + IPL, ganglion cell layer + inner plexiform layer; FAZ, foveal avascular zone; SCP, superficial capillary plexus; DCP, deep capillary plexus; FR, full retina; IR, inner ring; PD, perfusion density; AIS, area of intercapillary space.

associated with vessel closure, showing decreased VD ($p < 0.001$), decreased PD ($p < 0.001$), increased FAZ area ($p < 0.026$), and increased AIS ($p < 0.001$). Phenotype C, identified according to decreased VD metrics, also showed increased MAT values ($p < 0.001$), confirming the predominant microvascular damage that identifies this phenotype and confirming general agreement between the old and new classification of phenotype C. It is relevant that the differences between the two phenotypes at baseline reach a highly statistical significance level in almost all OCTA metrics of microvascular disease variables. However, neurodegenerative changes, represented by GCL + IPL thinning, do not show differences between the two phenotypes.

The overall 2-year progression of the study population (Table 2) showed only alterations in the blood lipid levels. The ocular characteristics showed a progressive thinning of the GCL + IPL ($p < 0.001$) and decrease in VD of the DCP ($p = 0.047$), associated with an increase in AIS in the DCP ($p = 0.040$). Over the 2-year period, the PD decreased in the SCP and in the FR (PD, SCP = 0.001; PD, FR = 0.011).

When comparing the ocular markers of phenotypes B and C after 1 year of follow-up, there was a significant thinning in the GCL + IPL layers in both phenotypes, which is more apparent in phenotype C (Table 3). Decreased PD was present mainly in phenotype B (PD-DCP, $p < 0.001$). Phenotype B also showed increased AIS, preferentially located in the DCP ($p = 0.001$).

Evaluation of the ocular variables of phenotypes B and C after 2 years (V4) of follow-up revealed also differences in the 2-year progression of the two phenotypes (Table 3). Both phenotypes, B and C, presented significant progression in GCL + IPL thinning ($p < 0.001$), reinforcing the presence of a DR associated neurodegenerative process in these individuals. At the microvascular level, the finding of a decrease in PD in both SCP and DCP only in phenotype B is of relevance, suggesting that disease progression in phenotype B may be associated with a functional microvascular response involving vessel caliber changes

(Table 3). Finally, AIS increased during the 2-year follow-up in phenotype B, with apparent stabilization in the SCP and DCP of the IR of phenotype C.

During the 2-year period of follow-up, 23 eyes developed CIME. Phenotype B was preferentially associated with the development of CIME (31%) in comparison with phenotype C (5%). Twenty belonged to phenotype B and the other three to phenotype C (Table 4). Association with development of CIME was observed with the ocular imaging markers tested, particularly with increased CRT ($p < 0.001$) and smaller FAZ area ($p = 0.012$). Significant increases in VD ($p < 0.001$) and PD ($p < 0.001$), involving predominantly the DCP, occurred in eyes that developed CIME. These findings indicate an association between the presence of CIME and increased vessel volume in DCP.

Discussion

In this study, we have focused on the characterization of different patterns of disease progression of eyes with NPDR and only minimal, mild, or moderate ETDRS grades in a 2-year period. We analyzed the data comparing two risk phenotypes previously shown to be associated with disease progression and development of vision-threatening complications, phenotype C identified by active and progressive microvascular changes, and phenotype B identified by the presence of increased retinal thickening with minimal microvascular changes [3–5].

The study showed that these two phenotypes have different patterns of disease progression with different risks for development of vision-threatening complications. Development of CIME is preferentially associated with phenotype B, whereas progressive decrease of VD is associated with phenotype C. Interestingly, there were only two occurrences of CSME in the 2-year period of follow-up, with one occurring in an eye classified as phenotype B and other in one eye classified as phenotype C. Of interest is the fact that both these eyes showed predominantly changes in PD rather than in VD, indicating changes in flow rather than vessel closure [12].

Another relevant finding is the observation that retinal neurodegeneration is present in both phenotypes [13]. Retinal neurodegeneration appears to function as a trigger for the deficient microvascular response and development of microvascular closure in phenotype C and for the alteration of the blood-retinal barrier and edema (increased CRT) that characterizes phenotype B. The differ-

Table 3. Comparison of ocular characteristics between phenotypes at baseline (V1), V3 (12 months), and V4 (24 months), and progression on 1-year and 2-year follow-up separated by phenotype

	Baseline (V1 – 0M)			1 year (V3 – 12M)			2 years (V4 – 24M)			Progression phenotype B		Progression phenotype C	
	Phenotype B	Phenotype C	*p* value* (B vs. C)	Phenotype B	Phenotype C	*p* value* (B vs. C)	Phenotype B	Phenotype C	*p* value* (B vs. C)	*p* value§ (V1 vs. V3)	*p* value§ (V1 vs. V4)	*p* value§ (V1 vs. V3)	*p* value§ (V1 vs. V4)
Ocular characteristics, mean±SD													
BCVA, logMAR	0.00±0.08	0.03±0.09	0.218	0.03±0.10	0.04±0.09	0.574	0.04±0.12	0.02±0.10	0.592	**0.011**	**0.012**	0.381	0.954
CRT, µm	285.57±13.09	268.81±21.81	**<0.001**	287.48±22.48	270.16±22.33	**<0.001**	290.17±26.96	267.84±21.03	**<0.001**	0.659	0.693	0.802	0.428
GCL + IPL thickness, µm	81.39±6.92	78.74±7.71	0.069	80.85±7.14	77.60±8.01	**0.032**	80.02±6.98	77.34±7.99	0.069	**0.003**	**<0.001**	**<0.001**	**<0.001**
FAZ circularity	0.60±0.10	0.58±0.11	0.529	0.60±0.11	0.57±0.09	0.093	0.61±0.09	0.60±0.08	0.368	0.853	0.914	0.390	0.608
FAZ area, mm^2	0.22±0.10	0.25±0.09	**0.026**	0.23±0.09	0.25±0.09	0.122	0.23±0.09	0.26±0.09	**0.016**	0.398	0.268	0.889	0.231
VD – IR – SCP, mm^{-1}	21.63±0.71	19.6±0.94	**<0.001**	21.29±1.02	19.93±1.26	**<0.001**	21.2±1.25	19.83±1.20	**<0.001**	**0.017**	**0.012**	0.068	0.088
VD – IR – DCP, mm^{-1}	16.78±1.60	14.82±2.22	**<0.001**	15.55±2.37	14.31±2.41	**0.013**	16.25±1.90	14.58±2.17	**<0.001**	**<0.001**	**0.021**	0.080	0.610
VD – IR – FR, mm^{-1}	23.25±0.73	21.43±0.97	**<0.001**	23.03±0.96	21.86±1.23	**<0.001**	22.93±1.08	21.78±1.18	**<0.001**	0.180	0.085	**0.003**	**0.010**
PD – IR – SCP	0.40±0.02	0.38±0.02	**<0.001**	0.39±0.02	0.38±0.02	**<0.001**	0.39±0.02	0.37±0.02	**<0.001**	**0.002**	**0.002**	0.230	0.136
PD – IR – DCP	0.32±0.03	0.29±0.04	**<0.001**	0.30±0.04	0.28±0.04	**0.025**	0.31±0.03	0.29±0.04	**<0.001**	**<0.001**	**0.029**	0.115	0.623
PD – IR – FR	0.43±0.02	0.40±0.02	**<0.001**	0.42±0.02	0.40±0.02	**<0.001**	0.42±0.02	0.40±0.02	**<0.001**	**0.018**	**0.012**	0.506	0.303
AIS – SCP (×1,000)	23.02±10.06	34.35±8.61	**<0.001**	24.89±10.78	35.46±12.36	**<0.001**	25.64±11.91	33.85±11.25	**<0.001**	0.054	**0.012**	0.655	0.340
AIS – DCP (×1,000)	39.25±14.11	48.43±14.36	**<0.001**	47.12±19.58	48.39±14.28	0.463	44.41±18.50	48.48±16.13	**0.020**	**<0.001**	**0.004**	0.917	0.944
AIS – FR (×1,000)	15.01±7.56	21.86±6.91	**<0.001**	16.08±9.01	23.10±10.00	**<0.001**	16.33±8.69	21.49±8.76	**<0.001**	0.160	**0.033**	0.708	0.315

Bold values represent statistically significant alterations with $p < 0.05$, using the * Mann-Whitney U test and the §Wilcoxon signed-rank test. SD, standard deviation; phen., phenotype; BCVA, best-corrected visual acuity; CRT, central retinal thickness; GCL + IPL, ganglion cell layer + inner plexiform layer; FAZ, foveal avascular zone; SCP, superficial capillary plexus; DCP, deep capillary plexus; FR, full retina; IR, inner ring; PD, perfusion density; AIS, area of intercapillary space.

Table 4. Comparison of systemic and ocular characteristics at V4 (24 months) between patients with CIME and no CIME

	CIME	No CIME	*p* value
Systemic characteristics, mean ± SD			
HbA1c, %	7.45±0.97	7.59±1.06	0.558
Total cholesterol, mg/dL	144.48±24.39	160.2±38.13	0.079
LDL cholesterol, mg/dL	72.48±23.65	84.42±30.67	0.110
HDL cholesterol, mg/dL	49.3±8.48	49.1±14.32	0.602
Triglycerides, mg/dL	112.96±39.62	143.74±74.84	0.073
Systolic blood pressure, mm Hg	139.43±21.21	141.98±11.13	0.097
Diastolic blood pressure, mm Hg	74.17±11.26	73.85±9.33	0.687
Ocular characteristics, mean ± SD			
BCVA, logMAR	0.05±0.12	0.03±0.11	0.626
CRT, µm	315.22±30.05	271.04±17.35	**<0.001**
GCL + IPL thickness, µm	80.55±6.66	78.53±7.71	0.293
FAZ circularity	0.59±0.1	0.61±0.08	0.543
FAZ area, mm^2	0.21±0.12	0.25±0.08	**0.012**
VD – IR – SCP, mm^{-1}	21.65±1.12	20.29±1.31	**<0.001**
VD – IR – DCP, mm^{-1}	16.99±1.53	15.1±2.2	**<0.001**
VD – IR – FR, mm^{-1}	23.35±0.91	22.16±1.2	**<0.001**
PD – IR – SCP	0.40±0.03	0.38±0.02	**0.001**
PD – IR – DCP	0.33±0.03	0.29±0.04	**<0.001**
PD – IR – FR	0.43±0.02	0.41±0.02	**0.001**
AIS – SCP (×1,000)	29.57±12.45	29.65±12.35	1.000
AIS – DCP (×1,000)	47.48±15.72	46.28±18.02	0.676
AIS – FR (×1,000)	19.10±9.72	18.75±8.99	0.871

Bold values represent statistically significant alterations with $p < 0.05$, using the Mann-Whitney U test. SD, standard deviation; HbA1c, glycated hemoglobin A1c; LDL, low-density lipoprotein; HDL, high-density lipoprotein; BCVA, best-corrected visual acuity; CRT, central retinal thickness; GCL + IPL, ganglion cell layer + inner plexiform layer; FAZ, foveal avascular zone; SCP, superficial capillary plexus; DCP, deep capillary plexus; FR, full retina; IR, inner ring; PD, perfusion density; AIS, area of intercapillary space.

ent phenotypes appear, indeed, to be the result of a different microvascular response in different patients to the neurodegenerative changes occurring in the retina as a result of chronic hyperglycemia and diabetes [14].

Phenotype C is characterized by more advanced microvascular changes well identified by OCTA metrics. It is relevant that although at baseline the SCP shows more occlusion, the 1-year progression registered in vessel closure shifted to the DCP. It appears that in the initial stages of DR, the capillary closure is better identified in the SCP and in the macular area, involving alteration of the FAZ, but progression in the initial stages of diabetic retinal vascular disease appears to occur through changes involving the DCP [12, 13, 15].

Skeletonized VD metrics have been considered to represent more permanent closure, whereas changes in flow, i.e., caliber changes, are represented by PD metrics [16]. Our observations showed alterations in PD, mainly in the earlier stages of DR, more specifically in ETDRS grade 35 and alterations in VD occurring predominantly in ETDRS grade 43–47 and in phenotype C. The possibility of discriminating which microvascular change predominates in a specific moment of disease progression may further contribute to identify the stage of the disease and its expected rate of progression.

It is of note that the results of OCTA metrics of the microvascular changes showed good consistency throughout the study with very good agreement between the results of skeletonized VD and AIS both representing vessel closure. These findings are in general agreement with other authors such as Terada et al. [17].

The results here reported, focusing on eyes with NPDR with signs of risk for progression [5], show that progression of the changes occurring in the retina, over a 2-year period, varies between different risk phenotypes demonstrating the complexity of DR progression. We were able to distinguish 2 groups of patients with different courses of disease progression. The observations here reported

indicate the need to combine information from different stages of the disease, as defined by ETDRS grading, with patterns of progression as characterized by risk phenotype classification [16].

Our findings offer an explanation for the conflicting results reporting preferential involvement of the SCP or the DCP in the initial stages of NPDR [15, 18, 19]. It is likely that different studies have included different proportions of eyes with different phenotypes.

Development of CIME occurred preferentially in phenotype B and was associated with changes in VD and PD involving preferentially the DCP. Vasodilation and capillary recruitment involving the DCP may play an important role in the development of the initial stages of diabetic macular edema [12].

A limitation of this study is the focus on the initial stages of DR, allowing conclusions to be made on 2-year progression of changes occurring only in eyes of people with T2D with mild or moderate DR. However, the use of these criteria guaranteed that the analysis is restricted to a population with NPDR, well before development of proliferative DR. Another limitation is the relatively small number of individuals included in the study and the rather restricted inclusion criteria, focusing on a population that is relatively well controlled without renal or cardiovascular diseases, but similar to the one usually enrolled in clinical trials to test new therapeutic options. However, the phenotype characterization and direct comparison between them is of major value and offers new insights into the complexity of diabetic retinal disease and of its progression and regression.

In summary, DR appears to be characterized by the presence of progressive neurodegenerative changes that in some patients lead to a deficient microvascular response characterized by progressive vascular closure and ischemia whereas in others involves preferentially the DCP and is apparently associated with an alteration of the blood-retinal barrier and increased thickening of the retina [13, 20, 21]. Diabetic retinal disease progresses through three main disease pathways, neurodegeneration, alteration of the blood-retinal barrier, and vascular closure. The predominance of one of these main disease pathways in an individual patient offers the possibility of different therapeutical strategies by addressing the dominant disease pathway [22].

The observations here reported offer intriguing and promising perspectives for personalized management of DR. After diagnosis of NPDR and still in the initial stages of retinal disease, different phenotypes can be identified through OCT and OCTA. These examinations are easy to perform and can be repeated easily without major inconvenience to the patient. This study confirms their value for improved characterization of individual disease progression allowing better identification of eyes at risk for progression and development of vision-threatening complications [14, 16]. The characterization of specific phenotypes is also an essential step when looking for genotype characterization of the eyes at risk [23].

The retinopathy phenotypes identified in people with T2D not only show different risks for vision-threatening complications, as demonstrated in previous studies, but also allow short-term identification and characterization of NPDR disease progression. Phenotype B is a relatively slow progression phenotype that appears to be adequately followed at relatively larger intervals, suggesting that examination intervals of 1 year are acceptable. On the other hand, people with T2D presenting phenotype C (characterized by vessel closure and ischemia) should receive frequent attention to follow closely the extent and progression of the ischemia and examinations may be needed at shorter intervals than 1 year. In conclusion, the data here presented reinforce the concept that the classification of retinopathy phenotypes in T2D individuals might be a useful tool to facilitate a more personalized approach to the management of diabetic retinal disease.

Statement of Ethics

The tenets of the Declaration of Helsinki were followed, and the study was reviewed and approved by the Ethics Committee of AIBILI with the number CEC/194/18 (CORDIS), NCT03696810 (ClinicalTrials.gov identifier). A written informed consent was signed by each participant, agreeing to participate in the study, after all procedures were explained.

Conflict of Interest Statement

Luísa Ribeiro, Inês Marques, Torcato Santos, Sara Carvalho, Ana Rita Santos, Luís Mendes, and Conceição Lobo have no conflicts of interest to declare. José Cunha-Vaz reports grants from Carl Zeiss Meditec and is a consultant for Alimera Sciences, Allergan, Bayer, Gene Signal, Novartis, Pfizer, Precision Ocular Ltd., Roche, Sanofi-Aventis, Vifor Pharma, and Carl Zeiss Meditec.

Funding Sources

This work was supported by AIBILI, COMPETE Portugal 2020, Foundation for Science and Technology (Project No.: 02/SAICT/2017-032412), and the Fundo de Inovação, Tecnologia e Economia Circular (FITEC) – Programa Interface (FITEC/CIT/2018/2).

Author Contributions

Luísa Ribeiro, Inês Marques, Torcato Santos, Sara Carvalho, Ana Rita Santos, and Luís Mendes collected data, analyzed, wrote, reviewed, and edited the manuscript. Conceição Lobo assisted in the analysis and interpretation of the data. José Cunha-Vaz is the guarantor of this work, as such, had full access to all the data in the study, and takes responsibility for the integrity of the data and the accuracy of the data analysis. All authors have read and agreed to the published version of the manuscript.

Data Availability Statement

All data generated or analyzed during this study are included in this article. Further inquiries can be directed to the corresponding author.

References

1 Cheung N, Mitchell P, Wong TY. Diabetic retinopathy. Lancet. 2010 Jul;376(9735):124–36.
2 Narayan KV, Boyle JP, Geiss LS, Saaddine JB, Thompson TJ. Impact of recent increase in incidence on future diabetes burden: U.S., 2005–2050. Diabetes Care. 2006 Sep;29(9):2114–6.
3 Nunes S, Ribeiro L, Lobo C, Cunha-Vaz J. Three different phenotypes of mild nonproliferative diabetic retinopathy with different risks for development of clinically significant macular edema. Invest J Ophthalmol Vis Sci. 2013;54(7):4595–604.
4 Cunha-Vaz J, Ribeiro L, Lobo C. Phenotypes and biomarkers of diabetic retinopathy. Prog Retin Eye Res. 2014 Jul;41:90–111.
5 Marques IP, Madeira MH, Messias AL, Santos T, Martinho AC-V, Figueira J, et al. Retinopathy phenotypes in type 2 diabetes with different risks for macular edema and proliferative retinopathy. J Clin Med. 2020 May;9(5):E1433.
6 Friedman SM, Almukhtar TH, Baker CW, Glassman AR, Elman MJ, Bressler NM, et al. Topical nepafenec in eyes with noncentral diabetic macular edema. Retina. 2015;35(5):944–56.
7 Ferris FL, Bailey I. Standardizing the measurement of visual acuity for clinical research studies: guidelines from the Eye Care Technology Forum. Ophthalmology. 1996;103(1):181–2.
8 Santos AR, Costa MÂ, Schwartz C, Alves D, Figueira J, Silva R, et al. Optical coherence tomography baseline predictors for initial best-corrected visual acuity response to intravitreal anti-vascular endothelial growth factor treatment in eyes with diabetic macular edema: the CHARTRES Study. Retina. 2018 Jun;38(6):1110–9.
9 Mendes L, Marques IP, Cunha-Vaz J. Comparison of different metrics for the identification of vascular changes in diabetic retinopathy using OCTA. Front Neurosci. 2021;15:755730.
10 Lei J, Durbin MK, Shi Y, Uji A, Balasubramanian S, Baghdasaryan E, et al. Repeatability and reproducibility of superficial macular retinal vessel density measurements using optical coherence tomography angiography en face images. JAMA Ophthalmol. 2017 Oct;135(10):1092–8.
11 Ribeiro L, Bandello F, Tejerina AN, Vujosevic S, Varano M, Egan C, et al. Characterization of retinal disease progression in a 1-year longitudinal study of eyes with mild nonproliferative retinopathy in diabetes type 2. Invest Ophthalmol Vis Sci. 2015 Aug;56(9):5698–705.
12 Ong JX, Fawzi AA. Perspectives on diabetic retinopathy from advanced retinal vascular imaging. Eye. 2022;36(2):319–27.
13 Madeira MH, Marques IP, Ferreira S, Tavares D, Santos T, Santos AR, et al. Retinal neurodegeneration in different risk phenotypes of diabetic retinal disease. Front Neurosci. 2021 Dec;15:800004.
14 Cunha-Vaz J. A central role for ischemia and OCTA metrics to follow DR progression. J Clin Med. 2021 Apr;10(9):1821.
15 Durbin MK, An L, Shemonski ND, Soares M, Santos T, Lopes M, et al. Quantification of retinal microvascular density in optical coherence tomographic angiography images in diabetic retinopathy. JAMA Ophthalmol. 2017 Apr;135(4):370–6.
16 Cunha-Vaz J, Mendes L. Characterization of risk profiles for diabetic retinopathy progression. J Pers Med. 2021 Aug;11(8):826.
17 Terada N, Murakami T, Uji A, Ishihara K, Dodo Y, Nishikawa K, et al. The intercapillary space spectrum as a marker of diabetic retinopathy severity on optical coherence tomography angiography. Sci Rep. 2022;12(1):3089.
18 Nesper PL, Roberts PK, Onishi AC, Chai H, Liu L, Jampol LM, et al. Quantifying microvascular abnormalities with increasing severity of diabetic retinopathy using optical coherence tomography angiography. Invest Ophthalmol Vis Sci. 2017;58(6):BIO307–15.
19 Sambhav K, Abu-Amero KK, Chalam KV. Deep capillary macular perfusion indices obtained with OCT angiography correlate with degree of nonproliferative diabetic retinopathy. Eur J Ophthalmol. 2017 Nov;27(6):716–29.
20 Santos T, Warren LH, Santos AR, Marques IP, Kubach S, Mendes LG, et al. Swept-source OCTA quantification of capillary closure predicts ETDRS severity staging of NPDR. Br J Ophthalmol. 2022 May;106(5):712–8.
21 Lobo C, Santos T, Marques IP, Madeira MH, Santos AR, Figueira J, et al. Characterisation of progression of macular oedema in the initial stages of diabetic retinopathy: a 3-year longitudinal study. Eye. 2022 Jan. Epub ahead of print.
22 Marques IP, Alves D, Santos T, Mendes L, Santos AR, Lobo C, et al. Multimodal imaging of the initial stages of diabetic retinopathy: different disease pathways in different patients. Diabetes. 2019 Mar;68(3):648–53.
23 Simões MJ, Lobo C, Egas C, Nunes S, Carmona S, Costa MÂ, et al. Genetic variants in ICAM1, PPARGC1A and MTHFR are potentially associated with different phenotypes of diabetic retinopathy. Ophthalmologica. 2014;232(3):156–62.